Self-induced transverse mode selection in a photorefractive extended cavity laser diode

Vincent Reboud, Nicolas Dubreuil, Pierre Fournet, Gilles Pauliat, Gérald Roosen, Daniel Rytz

Self-induced transverse mode selection in a photorefractive extended cavity laser diode

Vincent Reboud, Nicolas Dubreuil, Pierre Fournet, Gilles Pauliat, Gérald Roosen

Laboratoire Charles Fabry de l'Institut d'Optique, du Centre National de la Recherche Scientifique et de l'Université Paris-Sud, Bât. 503, Centre Scientifique d'Orsay, 91403 Orsay Cedex, France
nicolas.dubreuil@iota.u-psud.fr

Daniel Rytz

F.E.E. GmbH, Struthstr. 2, D-55743 Idar-Oberstein, Germany

Abstract: Previous works on photorefractive self-organizing laser cavities were about lasers that oscillate, prior the self-organization process occurs, on a set of axial modes sharing the same transverse structure. In a well-designed broad-area laser diode extended cavity, we theoretically and experimentally demonstrate that the insertion of a photorefractive crystal can also affect the transverse modal structure to force the laser, initially oscillating on several transverse modes, to oscillate on a single transverse and axial mode. This spatial self-organization process leads to an enhancement of the single mode operating range of the laser.

OCIS codes: (140.2020) Diode lasers; (140.3570) Lasers, single-mode; (160.5320) Photorefractive materials; (090.0090) Holography .

References and Links

1. S. Camacho-Lopez, M. J. Damzen, "Self-starting Nd: YAG holographic laser oscillator with a thermal grating," Opt. Lett. **24**, 753-755 (1999).
2. P. Sillard, A. Brignon, J. P. Huignard, "Loop resonators with self-pumped phase-conjugate mirrors in solid-state saturable amplifiers," J. Opt. Soc. Am. B **14**, 2049-2058 (1997).
3. M. Horowitz, R. Daisy, B. Fisher, "Filtering behavior of a self-induced three-mirror cavity formed by intracavity wave mixing in a saturable absorber," Opt. Lett. **21**, 299-301 (1996).
4. W. B. Whitten, J. M. Ramsey, "Mode selection in a continuous-wave dye laser with an intracavity photorefractive element," Opt. Lett. **12**, 117-119 (1987).
5. N. Huot, J. M. Jonathan, G. Pauliat, P. Georges, A. Brun, G. Roosen, "Laser mode manipulation by intracavity dynamic holography: Application to mode selection," Appl. Phys. B **69**, 155-157 (1999).
6. L. Meilhac, N. Dubreuil, G. Pauliat, G. Roosen, "Modeling of laser mode self-adapted filtering by photorefractive Fabry-Perot interferometers," Opt. Mater. **18**, 37-40 (2001).
7. S. Maerten, N. Dubreuil, G. Pauliat, G. Roosen, D. Rytz, and T. Salva, "Laser diode made single-mode by a self-adaptive photorefractive filter," Opt. Commun. **208**, 183-189 (2002).
8. A. Godard, G. Pauliat, G. Roosen, E. Ducloux, "Relaxation of the single-mode emission conditions in extended-cavity semiconductor lasers with a self-organizing photorefractive filter," Appl. Opt. **43**, 3543-3547 (2004).
9. J. M Verdiell, R. Frey, "A broad-area mode-coupling model for multiple-stripe semiconductor lasers," IEEE J. Quantum Electron. **26**, 270-279 (1990).
10. A. Yariv, *Quantum electronics* (Wiley, 1989), Chap. 19.
11. A. E. Siegman , *Lasers* (Mill Valley: University Science Books, 1986).
12. G. P. Agrawal, "Fast-Fourier-transform based beam-propagation model for stripe-geometry semiconductor lasers: Inclusion of axial effects," J. Appl. Phys. **56**, 3100-3109 (1984).
13. V. Reboud, *Cavités auto-organisables pour l'amélioration de la luminance des diodes laser de puissance*, PhD thesis, (Université Paris 11, Orsay, France, 2004).

#10349 - $15.00 USD Received 17 January 2006; revised 27 March 2006; accepted 27 March 2006

1. Introduction

Self-organizing laser cavities contain a dynamic holographic medium that plays the role of a modal filter. The oscillating modes record a common dynamic hologram, hologram that, in turn, acts as a filter for these modes. This filter, being self-adapted, does not require any adjustment and it adapts to any cavity change resulting, for instance, from a modification of the thermal loading and the cavity ageing. Such cavities have been built with various dynamic holographic media: thermal holograms recorded in a non-saturable absorbing medium [1], gain gratings recorded in solid-state amplifiers [2], absorption gratings recorded in a saturable absorber cell [3]. Another attractive solution consists in inserting a photorefractive crystal inside a laser cavity [4,5]. Considering that the reported cavities support a unique transverse modal structure, the reflective photorefractive Bragg grating recorded by the oscillating modes is one mirror of a Fabry-Perot whose second mirror is the cavity output coupler [6]. A self-organization, based on the mutual adaptation of this dynamic spectral filter to the oscillating modes, forces the steady-state oscillation on one axial mode.

The latter technique has been applied with diffraction limited laser diodes mounted in various extended cavities formed by the rear facet of the diode and a distant reflector. In a distant mirror based extended cavity around 810 nm, the insertion of a photorefractive Barium Titanate ($BaTiO_3$) crystal leads to a single axial mode operation over a wide injected current range without any other frequency filter [7]. Whereas the use of an intracavity photorefractive crystal in a tunable extended cavity relaxes the distant grating alignment constraints to avoid mode hopping [8].

All the reported cavities [4-8] support a unique transverse modal structure and the self-organizing process only occurs on the axial modes. Now we are interested in studying whether a similar process can act on the transverse modal structure of a laser. In fact, such an adaptive Fabry-Perot spectral filter is not expected to be selective enough to induce a spectral self-organization in a laser that initially oscillates on several transverse modes. Indeed, the frequency spacing between consecutive transverse modes is much smaller than the spacing between two modes in cavity sustaining a single transverse structure. The adaptive Fabry-Perot filter might not induce enough loss to neighboring modes. In order to fully understand the impact of the insertion of the photorefractive crystal inside a laser cavity that supports a plurality of transverse modes, one has to take into account the spatial distribution of the illumination pattern.

Suppose that the self-organizing process has forced the laser to oscillate in a single-mode, defined by a unique axial and transverse structure. The shape of the Bragg grating being recorded inside the photorefractive crystal perfectly matches the transverse structure of the oscillating mode. We will show in this paper that, for this mode, the light diffracted by the grating is optimally coupled back inside this mode. For other transverse modes, and if their phase profiles differ from that of the oscillating mode, the diffracted light is not well coupled back onto the modes. If these diffraction losses are important enough, the single transverse mode oscillation is a stable state. In addition, the Bragg grating in association with the output coupler of the cavity also acts as an adaptive spectral Fabry-Perot filter that selects a single axial mode. This process can only occur within cavities whose transverse modes greatly differ in their phase profiles. For instance, it cannot be efficient in cavities supporting Gaussian modes. Now, spatial self-organization might be present in extended cavities built with a non-diffraction limited laser diode for which the phase profiles of modes are very different from each others [9]. Hereafter, we study the modal feature of a broad-area laser (BAL) diode mounted in an extended cavity that contains no spatial filter except an intracavity photorefractive crystal. The cavity is made of the rear facet of a BAL diode, the front facet being anti-reflection coated, and of a distant mirror. Two lenses with adapted apertures are used to image without any filtering effect the BAL diode front facet onto the distant mirror. This cavity geometry is called hereafter “extended imaging cavity”. The presented work illustrates the capability of an intracavity photorefractive crystal to select transverse modes in this particular geometry of the extended cavity BAL diode. A model that depicts the modal

#10349 - $15.00 USD Received 17 January 2006; revised 27 March 2006; accepted 27 March 2006

behavior of this imaging cavity is presented in section 2. The setup and the experimental results are described in Section 3. Conclusion is given in Section 4.

2. Modeling of the modal behavior of a photorefractive extended imaging cavity

2.1 Photorefractive extended imaging cavity geometry

The extended imaging cavity that has been studied is depicted Fig. 1. The BAL diode is used as a pure amplifier, once its output facet is anti-reflection coated. A spherical lens L_1, with focal length equal to f_1, enables a perfect collimation of the beam along the fast axis (y dimension). The output facet of the BAL diode is imaged onto a $R = 10\%$ plane output mirror by using an additional cylindrical lens L_2 (with focal length equal to f_2). Neglecting the laser diode astigmatism, the non-apertured mirror is placed in the focal plane of second lens L_2. The distance between the lenses is set to $f_1 + f_2$.

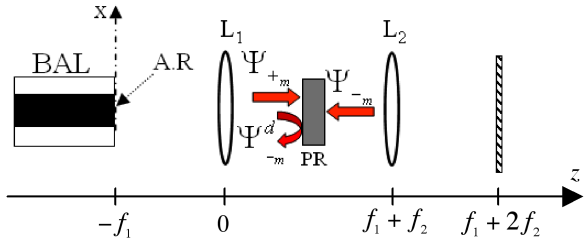

Fig. 1. Photorefractive extended imaging cavity BAL diode arrangement made of a intracavity photorefractive crystal and a distant plane mirror.

2.2 Model

Our simulations are based on the measured characteristics of a gain guided GaAs/GaAsAl double heterostructure BAL diode. Its gain zone width is 100 µm and it provides 2W output power in CW operating regime around 810 nm. In a first approximation, we assume an infinite absorption coefficient outside the gain zone boundaries. The transverse modes are then supposed to be perfectly confined inside the gain zone in which uniform refractive index and gain shapes are assumed. Temperature effects, carrier diffusion, spatial hole burning are neglected considering the rather low operating current being experimentally considered hereafter. As the eigen value problem of an infinite space well potential, a simple expression for the field distribution associated with the BAL diode transverse modes is then [9]:

$$\Psi_m(x) = \sqrt{\frac{1}{x_0}} \sin\left(\frac{m\pi x}{2x_0} + \frac{m\pi}{2}\right) \mathrm{rect}\left(\frac{x}{2x_0}\right), \tag{1}$$

where m refers to the mode number and x_0 is the half width of the BAL diode gain zone. The function "rect" is equal to 1 for $|x| < x_0$ and 0 elsewhere. The field is assumed to be linearly polarized along y direction.

The transverse structure of the extended imaging cavity modes coincide with those of the solitary BAL diode. We do assume that wave propagation through the semiconductor optical amplifier can only be done through the transverse modes Ψ_m. Typically, a 100µm width BAL diode contains 10 transverse modes [9]. Our analysis does not take into account the spatial BAL gain dependences: the transverse modes are supposed to experience the same gain value. A photorefractive crystal (PR) is inserted inside this extended cavity between L_1 and L_2, at a distance z from lens L_1 (see Fig. 1).

Our analysis consists in studying the stability of a single transverse mode oscillation in the extended imaging cavity BAL diode described in Fig. 1. Let us assume that only one single transverse mode m oscillates for which Ψ_{+m} (respectively Ψ_{-m}) is associated with the wave that propagates in the direction $z > 0$ (respectively $z < 0$) in the extended cavity. The

#10349 - $15.00 USD Received 17 January 2006; revised 27 March 2006; accepted 27 March 2006

interference inside the photorefractive crystal between waves Ψ_{+m} and Ψ_{-m} records a hologram whose $\pi/2$ phase shifted refractive index pattern is proportional to the interference modulation ratio [10]. By correctly setting the crystal orientation in the cavity, a growth of Ψ_{-m} is expected at the expense of Ψ_{+m} [10]. In other words, the diffracted part Ψ_{-m}^{d} of wave Ψ_{+m} interferes constructively with wave Ψ_{-m} and induces a reduction of the single lasing mode loss. Now, losses for the other non-lasing transverse modes are affected by the hologram because the wavefront of the diffracted wave Ψ_{-n}^{d} differs from the wave fronts of wave Ψ_{-n}. The effect of the hologram is strongly correlated to the difference between the wavefront associated with each transverse mode and it should depend on the position of the crystal inside the cavity.

In order to determine the effect of the hologram on the transverse modes, and especially on their losses, one has to evaluate the complex interference modulation ratio associated with the transverse mode *m* that is given by:

$$M_m(x,z) = \frac{2\,\Psi_{+m}^{*}(x,z)\cdot\Psi_{-m}(x,z)}{\Psi_{+m}(x,z)\cdot\Psi_{+m}^{*}(x,z)+\Psi_{-m}(x,z)\cdot\Psi_{-m}^{*}(x,z)}. \tag{2}$$

Its evaluation requires the calculation of the axial and transverse mode field dependence $\Psi_m(x,z)$ for the ten transverse modes. This calculation can ever be performed using a Fresnel integral calculation [11] or using the technique of the beam propagation method [12]. We have checked the validity of the paraxial approximation for this calculation. It allows the determination of the corresponding interference ratios inside the cavity. The output mirror reflectivity *R* has been chosen such as the complex interference modulation ratio is weak and considered constant along z in the presence of a hologram ($R = 10\%$). We consider now the hologram recorded by the single lasing mode *m*. Considering that the grating has a weak efficiency, the diffracted part $\Psi_{-n}^{d}(x,z)$ of a reading wave $\Psi_n(x,z)$ on the recorded hologram is proportional to the modulation ratio. It can be shown that [10]:

$$\Psi_{-n}^{d}(x,z) = \frac{\Gamma L}{4} M_m(x,z)\Psi_{+n}(x,z), \tag{3}$$

where Γ is the photorefractive gain and *L* the crystal thickness. The diffraction efficiency does not depend on the mode number but the losses induced by the hologram do. Indeed, considering that in an imaging cavity the two-conterpropagating waves are phase conjugated, we get $\Psi_{-m}(x,z) = r.\Psi_{+m}^{*}(x,z)$, with *r* the distant mirror amplitude reflectivity. Reporting Eq. (2) into Eq. (3), one concludes that for the lasing mode *m*, the diffracted wave Ψ_{-m}^{d} exactly overlaps wave Ψ_{-m}. Moreover, because of the photorefractive crystal orientation, these two waves Ψ_{-m}^{d} and Ψ_{-m} interfere constructively. Consequently the hologram does not affect the lasing mode field distribution, it only reduces the loss experienced by this mode. For the other non-lasing mode, waves Ψ_{-n}^{d} diffracted onto the recorded hologram differ from waves Ψ_{-n}. This imperfect overlapping results in additional losses for these modes. In order to quantify these losses, we compute the following overlapping coefficient, which represents, for mode *n*, the amplitude reflectivity of the output coupler formed by the recorded hologram and the distant mirror:

$$r_n = r + \frac{\int \Psi_{-n}^{d}(x,z).\Psi_{-n}^{*}(x,z)\,dx}{\int \Psi_{-n}(x,z).\Psi_{-n}^{*}(x,z)\,dx}. \tag{4}$$

We have considered in Eq. (4) that the amplitude of the wave during its transmission through the crystal is almost not affected thanks to the weak grating efficiency assumption. As explained above, in presence of a hologram recorded by a mode *m*, the amplitude reflectivity

#10349 - $15.00 USD Received 17 January 2006; revised 27 March 2006; accepted 27 March 2006

of the output coupler given by Eq. (4) is expected to strongly depend on the shape of the reading mode *n*.

2.3 Modeling results

Suppose that the hologram has been recorded by the single transverse lasing mode $m=1$. This assumption is justified by our experimental observations on the solitary BAL diode being used in our set-up that systematically show lasing oscillation firstly supported by a $m=1$ transverse mode. As it is shown in the next section, these observations continue to be valid in the extended imaging cavity configuration without any PR crystal. The transverse mode $m=1$ can be considered as the fundamental mode, meaning it is the lowest loss mode. For each reading mode *n*, the normalized reflectivity imposed by the output coupler, defined by the ratio $|r_n|^2 / |r_{m=1}|^2$, is calculated.

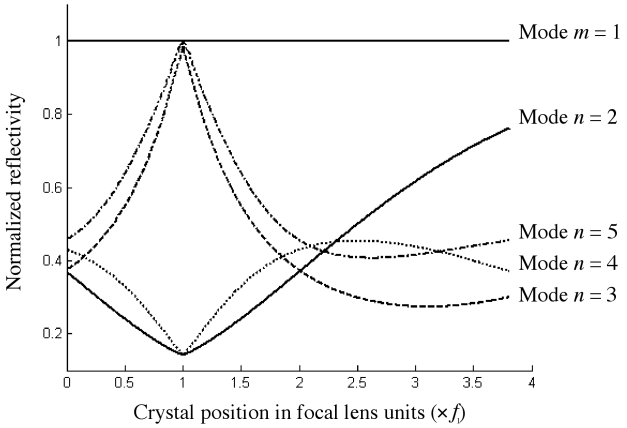

Fig. 2. Normalized reflectivity for modes $m=1, n=2,\cdots 5$ of the system composed by plane output cavity mirror and a hologram recorded by $m=1$.

We present in Fig. 2 its evolution for the first five modes versus the position of a photorefractive crystal inside the cavity. The product ΓL is taken equal to 1, which is the typical value for the $BaTiO_3$:Co we used in the experimental demonstration. For most of the crystal positions, the reflectivity of the lasing mode is higher than the reflectivity of any non-lasing transverse modes. This difference is only due to the presence of the recorded hologram. In the focal plane of the lens L_1, at $z = f_1$, all the wave fronts are plane and the discrimination observed between even and odd transverse modes comes from their fixed phase shift equal to $\pi/2$. Each mode is characterized by its transverse structure (*n* parameter) and its absolute position in frequency. Among all possible frequencies for modes $n=2,\cdots 5$ used in Fig. 2, we have chosen the frequencies, which are the closest to the frequency of the oscillating mode $m=1$. For the other crystal positions, the transverse modes differ from their wavefront structure, resulting in strong disparities in terms of reflectivity values. The strongest discrimination between modes $m=1$ and $n\neq 1$ occurs at $z=0$ and $z=2f_1$. For these crystal positions, the reflectivity seen by non-lasing modes is approximately 2.5 lower than the reflectivity seen by the lasing mode. As mentioned in introduction the spectral selectivity effect of the holographic filter is less efficient in that situation because the spectral interval between two successive modes is very small [6]. This theoretical result demonstrates the capability of an intracavity photorefractive crystal to introduce strong loss disparities between transverse modes. The hologram being adapted to a particular transverse lasing mode acts as an efficient spatial filter.

The loss discrimination induced by the hologram can be also understood by a visual inspection of the interference pattern. Therefore, we plotted in Fig. 3 the modulus of the

#10349 - $15.00 USD Received 17 January 2006; revised 27 March 2006; accepted 27 March 2006

modulation ratios (Eq. (2)) of the first four transverse modes, $m=1$ to 4, around $z=2f_1$. These four modulation ratio patterns present strong disparities between them. These images give an information on the strong disparities between the wavefronts of the different transverse modes. Note that the patterns drawn in Fig. 3 strongly depend on z position.

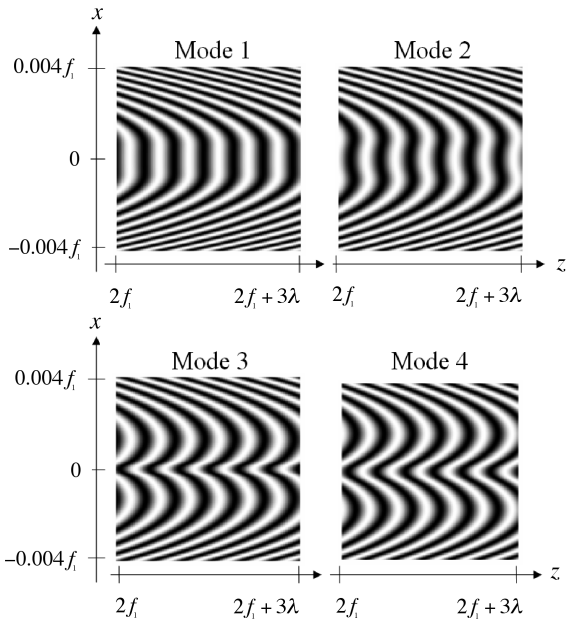

Fig. 3. Modulus of interference modulation ratio associated with the transverse modes *m=1,2,3,4* plotted around $z=2f_1$.

Such a holographic filter increases the difference of losses between the lasing transverse mode and the other ones. It extends the single transverse mode operating range of the extended cavity BAL diode. In addition, it does not induce additional detrimental losses for the initially lasing mode, contrary to techniques that use an intracavity-blocking filter. In that configuration, the fundamental transverse mode $m=1$ is of particular interest because it is the one that gives the best beam quality (see Eq. (1)). Calculations of normalized reflectivities were also conducted with sinusoids truncated by a Gaussian function. The dependences versus crystal position are comparable with both mode distributions. The discrimination ratio between the lasing mode and non-lasing modes is identical at the crystal position $z=0$ or $z=2f_1$. So, the value 2.5 of this coefficient is not strongly affected by the choice of mode distributions. On the assumption that the modes experience a unique gain value, the oscillation of a single transverse mode $m=1$ is then stable, the initial set of non-lasing modes being kept under the threshold level thanks to the hologram.

Finally, we expect this value to increase the single mode operation of the extended cavity BAL diode thanks to the hologram being recorded by the fundamental $m=1$ mode. We have experimentally investigated this point in the next section.

3. Experimental setup and results

3.1 Setup

The geometry of the laser cavity we have experimentally used is depicted in Fig. 4. The gain zone is made of an anti-reflection coated BAL diode, oscillating around 810 nm. Although the beam shape along *y* direction is diffraction limited, this is not the case along the transverse

#10349 - $15.00 USD Received 17 January 2006; revised 27 March 2006; accepted 27 March 2006

direction, *x* direction (see Fig. 4), the width of the gain zone being equal to 100 μm. The transverse confinement is obtained through gain-guided effect that exhibits a propagation through a set of approximately ten transverse modes. An aspheric lens with a 2.75 mm focal length (f_1) is set to collimate the beam along the *y* direction. The beam is coupled back into the BAL diode after reflection on a $R=|r|^2=10\%$ plane mirror. A 7.7 mm focal length (f_2) cylindrical lens is placed between the aspheric lens and the plane mirror. Finally, a $BaTiO_3$:Co photorefractive crystal with a thickness $L=2.1$ mm and a gain $\Gamma=480$ m^{-1} is inserted between the aspheric lens and the cylindrical lens. The optical distance between the two lenses is set equal to f_1+f_2 taking into account the crystal thickness. The crystal is put close to the aspheric lens, in order to obtain a strong discrimination between modes, as predicted by the numerical analysis (Fig. 2). The crystal is oriented so that diffracted wave Ψ_{-m}^{d} interferes constructively with wave Ψ_{-m}. A slight adjustment of the distance between the cylindrical lens and the mirror is required to compensate the astigmatism of the laser diode. Coupling of the beam into the gain zone, after one round trip in the extended cavity, is then optimized.

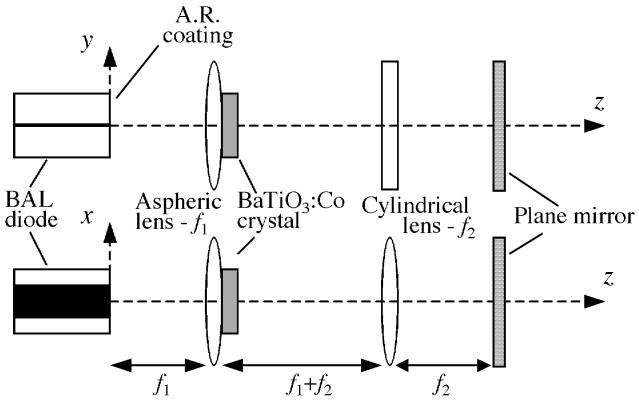

Fig. 4. Photorefractive extended imaging cavity broad area laser diode made of a 10 % distant plane mirror, an aspheric and a cylindrical lenses, and a $BaTiO_3$:Co photorefractive crystal.

The near and the far field intensity distributions are monitored by two monochrome CCD cameras with respect to the plane of external mirror and thus to the output facet of the BAL diode. The output power is measured by a calibrated p-i-n photodetector. Finally, a 6 pm resolution spectrometer and a confocal Fabry-Perot interferometer are used to control the single or multi-mode operation of the laser source.

3.2 Experimental results

In order to understand the modal behavior of the extended imaging cavity without any photorefractive crystal and close to the threshold, the output facet of the BAL diode is imaged onto the input slit of the spectrometer. A spectrally dispersed image of the input slit obtained through the spectrometer is imaged onto a CCD camera. A set of four images is presented in Fig. 5, corresponding to four different injected currents around threshold. They give a spectrally resolved image of the intensity distribution at the output facet. This technique enables us to clearly identify the transverse structure of the oscillating modes. With the help of the Fabry-Perot interferometer we are able to clearly identify the single or multimode regimes of the laser.

Just above threshold (Fig. 5(a)), a $m=1$ fundamental mode appears with a weak output power equal to 3.5 mW. Single mode operation stops for $I=1.01I_{th}$. The emitted power is shared among three modes: two axial modes with the same $m=1$ profile, a powerful and a weaker one, and a third one with a $m=2$ profile (Fig. 5(b)). The output power is then equal to

#10349 - $15.00 USD Received 17 January 2006; revised 27 March 2006; accepted 27 March 2006

5 mW. First of all, it is noted that discrimination between the modes is very weak. Indeed the shape of the fundamental mode does not permit the complete saturation of the gain zone, which allows the appearance of higher order modes. At $I = 1.015 I_{th}$ (Fig. 5(c)), the emission is clearly bi-mode. At $I = 1.02 I_{th}$ (Fig. 5(d)), the laser oscillates on several axial modes of which the transverse structures correspond to modes $m = 1$ and $m = 2$. Comparison with the transmission spectrum of the scanning Fabry-Perot interferometer confirms this interpretation of the spectra of Fig. 5.

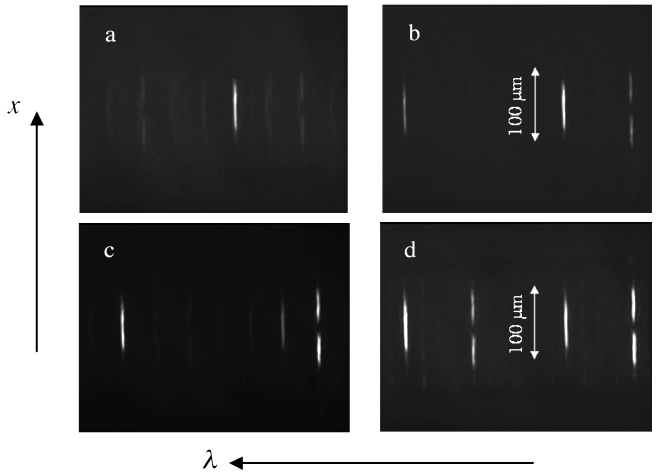

Fig. 5. Spectrally resolved near-field intensity distribution with the extended imaging cavity for several injection currents: (a) $I/I_{th} = 1.005$ (3.5 mW), (b) $I/I_{th} = 1.01$ (5 mW), (c) $I/I_{th} = 1.015$ (6.6 mW), (d) $I/I_{th} = 1.02$ (8.1 mW).

In a second set of experiments, we inserted the photorefractive crystal in the cavity. Then, the length of the cavity is adjusted in order to obtain again the imaging cavity. Table 1 compares the performance of the laser achieved without and with the crystal in terms of maximum output power obtained in the single mode operation, corresponding spatial beam quality M_x^2 along x direction, and brightness. In the transverse direction, the beam is diffraction limited. At the threshold, the factor M_y^2 of this beam is measured at a value close to 1. It remains almost constant when the current grows. The factor M_x^2 is evaluated through $1/e^2$ beam width measurements [11]. With an intracavity photorefractive crystal, a clear improvement of the operating range over which the laser is single mode is demonstrated. Results of Table 1 show that, thanks to the photorefractive crystal, the output power emitted in a single mode and the beam brightness are multiplied by a factor 9. We note that the factor M_x^2 measured at $1/e^2$ remains almost unchanged. We think that the slight difference is only due to the optical quality of crystal surfaces that could be easily improved. The near-field and the far-field intensity distributions are measured with and without crystal with the respect to the plane of output mirror. Figure 6(a) (respectively Fig. 6(b)) presents the far-field and near-field distributions without the intracavity crystal (respectively with the intracavity crystal).

#10349 - $15.00 USD Received 17 January 2006; revised 27 March 2006; accepted 27 March 2006

Table 1. Performances of the emitted beam in the single mode operation obtained without and with an intracavity photorefractive crystal.

	P (mW)	$M_x^2(1/e^2)$	Brightness ($MW.cm^{-2}.sr^{-1}$)
Without PR crystal	3.5	1.20	0.46
With PR crystal	33.7	1.25	4.21

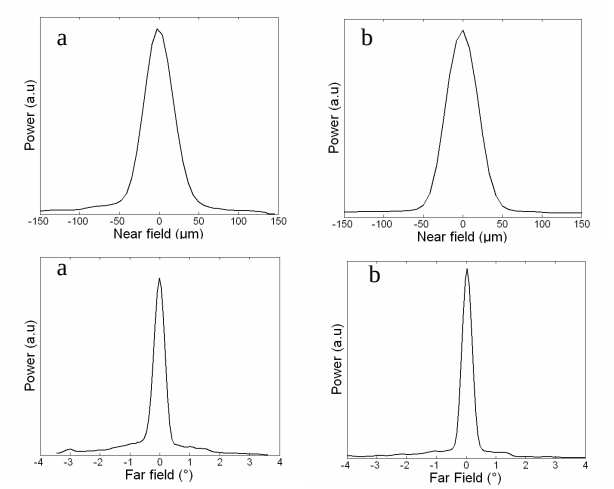

Fig. 6. Near-field and the far-field intensity distributions of emitted beam by the extended imaging cavity broad-area laser diode without the intra-cavity photorefractive crystal (a) at an output power of 3.5 mW and with the intra-cavity photorefractive crystal (b) at an output power of 33.7 mW.

4. Conclusion

We have theoretically demonstrated that the insertion of a photorefractive crystal in an extended cavity broad-area laser diode increases the losses for the non-lasing transverse modes without inducing additional loss for the lasing mode conversely to what happens with the use of a blocking filter. This extends the operating range over which this extended cavity is single mode. Although our numerical analysis has only been done on the transverse mode structure, note that the photorefractive crystal with the distant mirror also acts as a frequency self-adapted filter, like in [5-8]. We have experimentally demonstrated this self-adapted filter to also make a selection on the axial modes that lead to a single transverse and axial oscillation of this extended cavity BAL diode with a single-mode emission up to 33.7 mW. That corresponds to a brightness improvement by a factor 9, compared to a situation without photorefractive crystal. A complete numerical simulation that takes into account the gain guiding properties, like spatial hole burning and carrier diffusion, of the BAL diode has been conducted in [13]. This simulation confirms the spatial filtering effect induced by the intracavity photorefractive crystal and gives a good prediction of the single mode operating range. Above an output power of 33.7 mW, the laser is no more single-mode and oscillates on higher-order transverse and axial modes. The refractive hologram being recorded inside the photorefractive crystal is then no more efficient and an additional filter is required to maintain a single-mode oscillation with a greater output power. We will use this technique in other extended cavity geometries, which include static filters, in order to extend the output power in a single-mode operation with this kind of laser diode.

#10349 - $15.00 USD Received 17 January 2006; revised 27 March 2006; accepted 27 March 2006